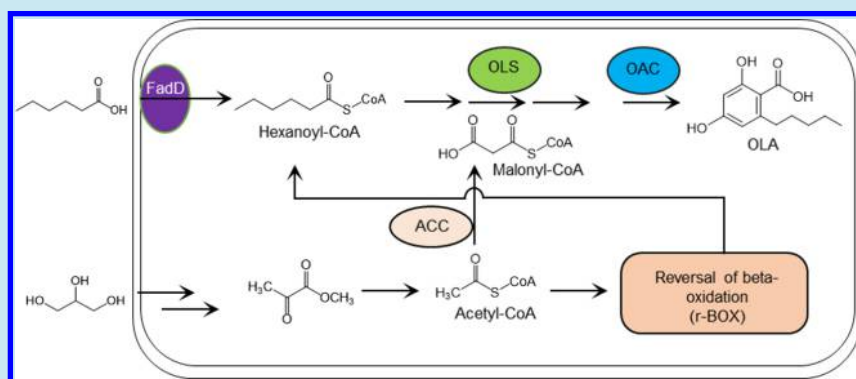


Synthetic Pathway for the Production of Olivetolic Acid in *Escherichia coli*

Zaigao Tan,[†] James M. Clomburg,[†] and Ramon Gonzalez^{*,†,‡,§}[†]Department of Chemical and Biomolecular Engineering, Rice University, Houston, Texas 77005, United States[‡]Department of Bioengineering, Rice University, Houston, Texas 77005, United States**S** Supporting Information

ABSTRACT: Type III polyketide synthases (PKS IIIs) contribute to the synthesis of many economically important natural products, most of which are currently produced by direct extraction from plants or through chemical synthesis. Olivetolic acid (OLA) is a plant secondary metabolite sourced from PKS III catalysis, which along with its prenylated derivatives has various pharmacological activities. To demonstrate the potential for microbial cell factories to circumvent limitations of plant extraction or chemical synthesis for OLA, here we utilize a synthetic approach to engineer *Escherichia coli* for the production of OLA. *In vitro* characterization of polyketide synthase and cyclase enzymes, OLA synthase and OLA cyclase, respectively, validated their requirement as enzymatic components of the OLA pathway and confirmed the ability for these eukaryotic enzymes to be functionally expressed in *E. coli*. This served as a platform for the combinatorial expression of these enzymes with auxiliary enzymes aimed at increasing the supply of hexanoyl-CoA and malonyl-CoA as starting and extender units, respectively. Through combining OLA synthase and OLA cyclase expression with the required modules of a β -oxidation reversal for hexanoyl-CoA generation, we demonstrate the *in vivo* synthesis of olivetolic acid from a single carbon source. The integration of additional auxiliary enzymes to increase hexanoyl-CoA and malonyl-CoA, along with evaluation of varying fermentation conditions enabled the synthesis of 80 mg/L OLA. This is the first report of OLA production in *E. coli*, adding a new example to the repertoire of valuable compounds synthesized in this industrial workhorse.

KEYWORDS: type III polyketide synthases (PKS III), olivetolic acid (OLA), synthetic biology, natural products

A broad diversity of natural products can be synthesized by type III polyketide synthases (PKS IIIs).^{1,2} Many of these products have been found to benefit human health, with PKS III products and derivatives garnering significant research interest in recent years.^{1,2} For instance, anthocyanins, the water-soluble pigments from mulberry fruits, have been reported to be useful in treating obesity, inflammation and cancer.³ Hyperforin, which is one of the primary active constituents from extracts of *Hypericum perforatum*, can be used for the treatment of depression.¹ The monoaromatic compound olivetolic acid (OLA), a member of the PKS III product class, holds promise for its pharmacological properties such as antimicrobial, cytotoxic, and photoprotective activities.^{2,4} In addition, OLA is a central intermediate in the synthesis of an important class of pharmacological compounds, as it serves as the alkylresorcinol moiety during the biosynthesis of cannabinoids, a class of

products that are becoming increasingly important due to their numerous pharmacological properties.^{5–7}

Currently, the production of OLA and its derivatives is primarily through direct extraction from plants.^{4,8,9} However, given that plants grow slowly and require at least several months for the accumulation of these compounds, direct extraction suffers from long cycles.¹⁰ While plant biotechnology offers the opportunity to improve natural product synthesis in native species, it is difficult to precisely control the expression level of transgenes in plants and adapt to industrial-scale production.¹¹ While the chemical synthesis of OLA is another alternative that has recently been reported,¹² the structural complexity of most natural products dictates inherent inefficiencies with total

Received: February 17, 2018

Published: July 5, 2018

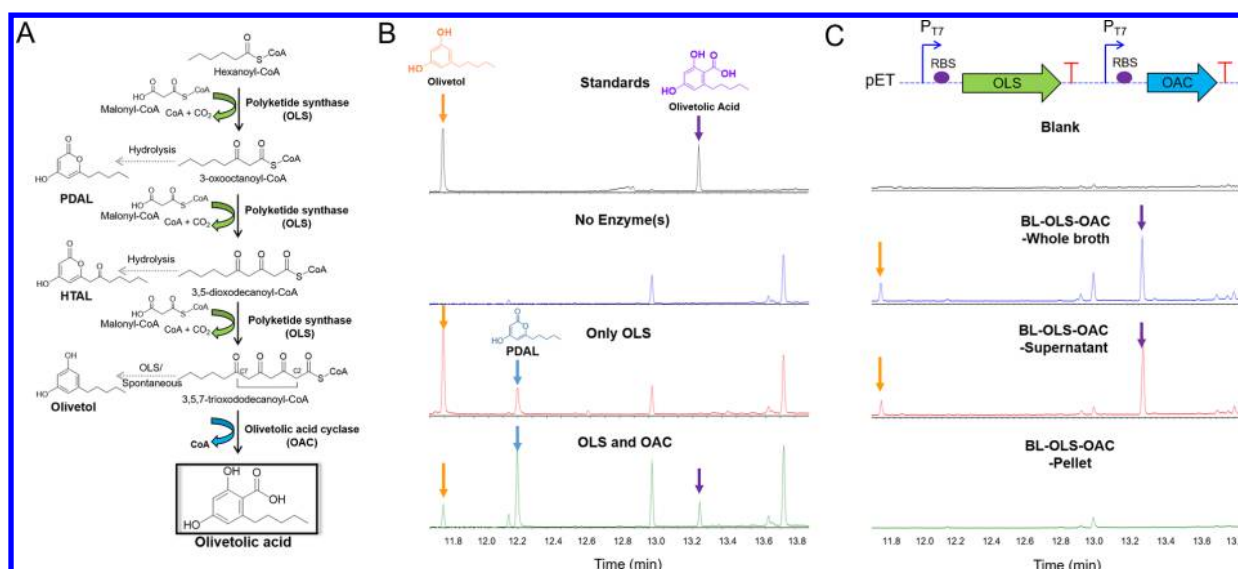


Figure 1. Production of olivetolic acid (OLA) by recruiting OLS and OAC. (A) Biosynthetic pathway of OLA from hexanoyl-CoA. Three malonyl-CoA extender units are added to the hexanoyl-CoA primer to form OLA through the Claisen condensation catalyzed by OLS and C2–C7 aldol cyclization catalyzed by OAC. Potential pathway byproducts, e.g., PDAL, HTAL and olivetol, can also be formed through hydrolysis of intermediate CoAs or spontaneous cyclization without carboxyl group retention. (B) *In vitro* production of OLA using recombinant and purified OLS and OAC core enzymes. Detailed MS identification of these OLA and byproducts can be seen in Figure S2. (C) *In vivo* production of OLA from resting cells biotransformations with *E. coli* BL21 (DE3). *E. coli* cells with the induced OLS and OAC from LB medium were collected and resuspended in fresh M9Y medium + 2% (wt/v) glucose with 4 mM hexanoate, and cultured at 22 °C for 48 h. Blank, BL21 (DE3) with pETDuet-1 empty vector. PDAL, pentyl diacetic acid lactone, HTAL, hexanoyl triacetic acid lactone.

chemical synthesis, which suffers from low yield and high energy waste.¹³ In contrast to these approaches, construction of microbial cell factories for production of these value-added plant natural products is a promising strategy.^{13–16}

Despite the structural complexity of the end product, the starting and extending units for polyketide biosynthesis are often tractable acyl-coenzyme A (CoA) intermediates. In the case of OLA biosynthesis, 3 iterations of 2-carbon additions (*via* decarboxylative condensation with malonyl-CoA as the donor) to an initial hexanoyl-CoA primer results in the formation of 3,5,7-trioxododecanoyl-CoA, which can be subsequently cyclized to form OLA (Figure 1). While it was initially thought that the polyketide synthase (OLS) from *C. sativa* was solely responsible for OLA biosynthesis, recombinant OLS was found to only synthesize olivetol, the decarboxylated form of OLA.¹⁷ It has since been shown that olivetolic acid biosynthesis requires a polyketide cyclase, *i.e.*, OLA cyclase (OAC), in addition to OLS, which catalyzes a C2–C7 intramolecular aldol condensation of the 3,5,7-trioxododecanoyl-CoA intermediate with carboxylate retention.¹⁸ Expression of OLS and OAC in *Saccharomyces cerevisiae*, along with feeding of sodium hexanoate, enabled the synthesis of 0.48 mg/L olivetolic acid in a 4 day fermentation.¹⁸ This represents a promising first step toward the development of microbial cell factories for the production of OLA that can be built upon to improve product synthesis from biorenewable feedstocks.

A potential bottleneck in improving product synthesis in *S. cerevisiae* is compartmentalization of acetyl-CoA metabolism, which results in the requirement for significant engineering efforts for the production of acetyl-CoA-derived products.¹⁹ Given the need for hexanoyl-CoA and malonyl-CoA in OLA synthesis, which are both commonly derived from acetyl-CoA, here we explored the possibility of engineering *Escherichia coli* for OLA production. In addition to its well-known physiology, metabolic network, and the ease of genetic manipulation, *E. coli*

has been engineered to produce a wide range of products from the acetyl-CoA node, including those derived directly from malonyl-CoA.^{19–22} We utilize a bottom-up, synthetic biology approach to develop a pathway for OLA production through testing and validating the required PKS and cyclase components in addition to auxiliary enzymes for generating the required precursors. Through the combinatorial expression of these enzymatic components with the required modules of a β -oxidation reversal pathway to supply hexanoyl-CoA,^{23,24} we demonstrate a functional biological pathway for the synthesis of OLA from a single carbon source and further identified precursor supply as a major limiting factor for product synthesis. The use of auxiliary enzymatic components aimed at increasing hexanoyl-CoA and malonyl-CoA and systematic metabolic engineering efforts enabled the synthesis of OLA at a titer of 80 mg/L, further demonstrating the viability of developing microbial cell factories for the synthesis of plant-based natural products.

RESULTS AND DISCUSSION

Recruiting OLS and OAC for Olivetic Acid Production. A synthetic pathway for olivetolic acid (OLA) biosynthesis in *E. coli* requires at least two catalytic enzymes, OLA synthase (OLS) and OLA cyclase (OAC).^{17,18} OLS is a type III PKS (tetraketide synthase) from *Cannabis* trichomes that catalyzes the formation of 3,5,7-trioxododecanoyl-CoA from a hexanoyl-CoA primer and 3 malonyl-CoA extender units *via* decarboxylative Claisen condensation.¹⁷ This 3,5,7-trioxododecanoyl-CoA intermediate can then be cyclized by OAC *via* C2–C7 intramolecular aldol condensation to form OLA.¹⁸ In addition to the desired product, evidence suggests that pathway byproducts, e.g., pentyldiacetic acid lactone (PDAL), hexanoyl triacetic acid lactone (HTAL) and olivetol can also be formed through hydrolysis of intermediate polyketide CoAs or spontaneous cyclization (Figure 1A).¹⁸

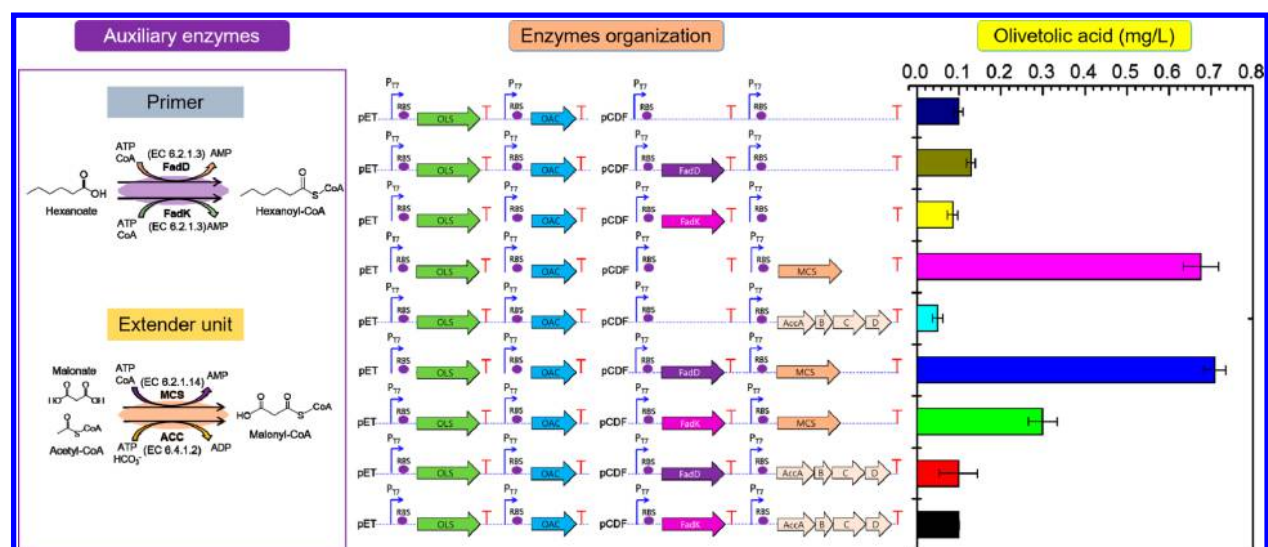


Figure 2. Impact of auxiliary enzymes for increasing hexanoyl-CoA and malonyl-CoA supply on olivetolic acid (OLA) production in BL21 (DE3). Left, auxiliary enzymes employed for increasing hexanoyl-CoA (FadD/FadK) and malonyl-CoA (MCS/ACC). FadD and FadK were employed to form hexanoyl-CoA from hexanoate and CoA. MCS and ACC can form the malonyl-CoA extender unit through two different mechanisms. Middle, enzyme organization of OLS/OAC core enzymes and FadD/FadK, MCS/ACC auxiliary enzymes. The vector expressing OLS and OAC was constructed using multiple cloning site 1 (Mcs1) and multiple cloning site 2 (Mcs2) of the pETduet-1 plasmid, respectively. FadD/FadK were constructed at the Mcs1 of pCDFduet-1 and MCS/ACC were constructed at the Mcs2 of pCDFduet-1. Right, OLA production using different combinations of auxiliary enzymes with OLS and OAC expression. *E. coli* cells expressing the indicated enzymes grown in LB medium were collected and resuspended in fresh M9Y medium with 2% (wt/v) glucose and 4 mM hexanoate. For strains harboring MCS, 12 mM malonate sodium was also included. Values represent the average of at least three biological replicates with error bars indicating standard deviation. FadD, long chain fatty acyl-CoA synthetase or ligase; FadK, short chain fatty acyl-CoA synthetase; MCS, malonyl-CoA synthetase; ACC, acetyl-CoA carboxylase.

To confirm the ability for OLS and OAC expressed in *E. coli* to synthesize OLA from hexanoyl-CoA and malonyl-CoA, in addition to evaluating potential byproducts, we conducted *in vitro* analysis of these enzymatic components (Figure 1B). Codon optimized, His-tagged OLS and OAC were expressed and purified from *E. coli* and utilized to determine product formation in a reaction system including hexanoyl-CoA (primer) and malonyl-CoA (extender unit). As seen in Figure 1B, incubation of OLS and OAC in the presence of these substrates resulted in OLA synthesis. Pathway byproducts PDAL and olivetol were also detected in samples with OLS only or including both OLS and OAC (Figure 1B). These byproducts were the only products formed in the absence of OAC (*i.e.*, assays with OLS only) confirming the indispensable nature of the OAC component for OLA formation.¹⁸

We next evaluated the ability to produce OLA *in vivo* through the construction of plasmid pET-P1-OLS-P2-OAC expressing codon-optimized versions of OLS and OAC. This plasmid was transformed into *E. coli* BL21 (DE3), both the OLS and OAC have soluble expression (Figure S1), and the resulting strain (BL-OLS-OAC) enabled the production of OLA following 48 h cultivation in biotransformation media with 4 mM hexanoate (Figure 1C). In addition to OLA, small amounts of olivetol were also detected, implying that while heterologous OAC cyclized the 3,5,7-trioxododecanoyl-CoA intermediate into OLA, the potential for byproduct formation is also a concern *in vivo*. It should be noted that even with the small amounts of OLA produced (~0.1 mg/L), this product was present in the fermentation broth (supernatant) instead of cell pellet (Figure 1C). The presence of OLA in supernatant might be due to export of OLA by a native *E. coli* transporter or from cell lysis.²⁵

Impact of Precursor Supply on Olivetolic Acid Production *In Vivo*. While the above results demonstrate the function of the required PKS and cyclase components *in vivo*, the

low OLA titers (~0.1 mg/L) (Figure 2) require additional assessment of the overall limitations for product synthesis. Given the functional expression and purification of OLS and OAC from *E. coli*, we reasoned a major limitation for OLA production is the availability of required precursors, opposed to issues with the expression or activity of these enzymes in *E. coli*. To determine the potential to improve product synthesis by increasing precursor supply, we expanded our synthetic approach through combinatorially expressing auxiliary enzymes for malonyl-CoA and/or hexanoyl-CoA generation with the OLS and OAC components.

For increasing malonyl-CoA supply, two classes of enzymes for biosynthesis of malonyl-CoA were evaluated. The first, malonyl-CoA synthetase (MCS) (EC 6.2.1.14), catalyzes the formation of malonyl-CoA from malonate, CoA and ATP.^{26,27} The MCS from *Bradyrhizobium japonicum*²⁷ was codon optimized and expressed in conjunction with OLS and OAC in *E. coli* supplied with 12 mM sodium malonate. Consistent with our hypothesis, increasing malonyl-CoA supply using this approach resulted in increased OLA titer, from 0.1 mg/L to 0.65 mg/L (*p*-value <0.05) (Figure 2). While this shows the importance of increasing malonyl-CoA supply, MCS requires the addition of exogenous malonate. To generate increased malonyl-CoA without malonate supplementation, we evaluated the overexpression of acetyl-CoA carboxylase (ACC) (EC 6.4.1.2) catalyzing the carboxylation of acetyl-CoA in the presence of ATP and bicarbonate (HCO_3^-). In *E. coli*, ACC consists of four different subunits, *e.g.*, AccA, AccB, AccC and AccD. Genes encoding the AccABCD complex were overexpressed (+ACC) in the BL-OLS-OAC strain (resulting in BL-OLS-OAC-ACC). However, the engineered +ACC strain did not improve OLA production in the absence of malonate (Figure 2). ACC requires acetyl-CoA as catalytic substrate, which is one of the most important central metabolites in *E. coli*,

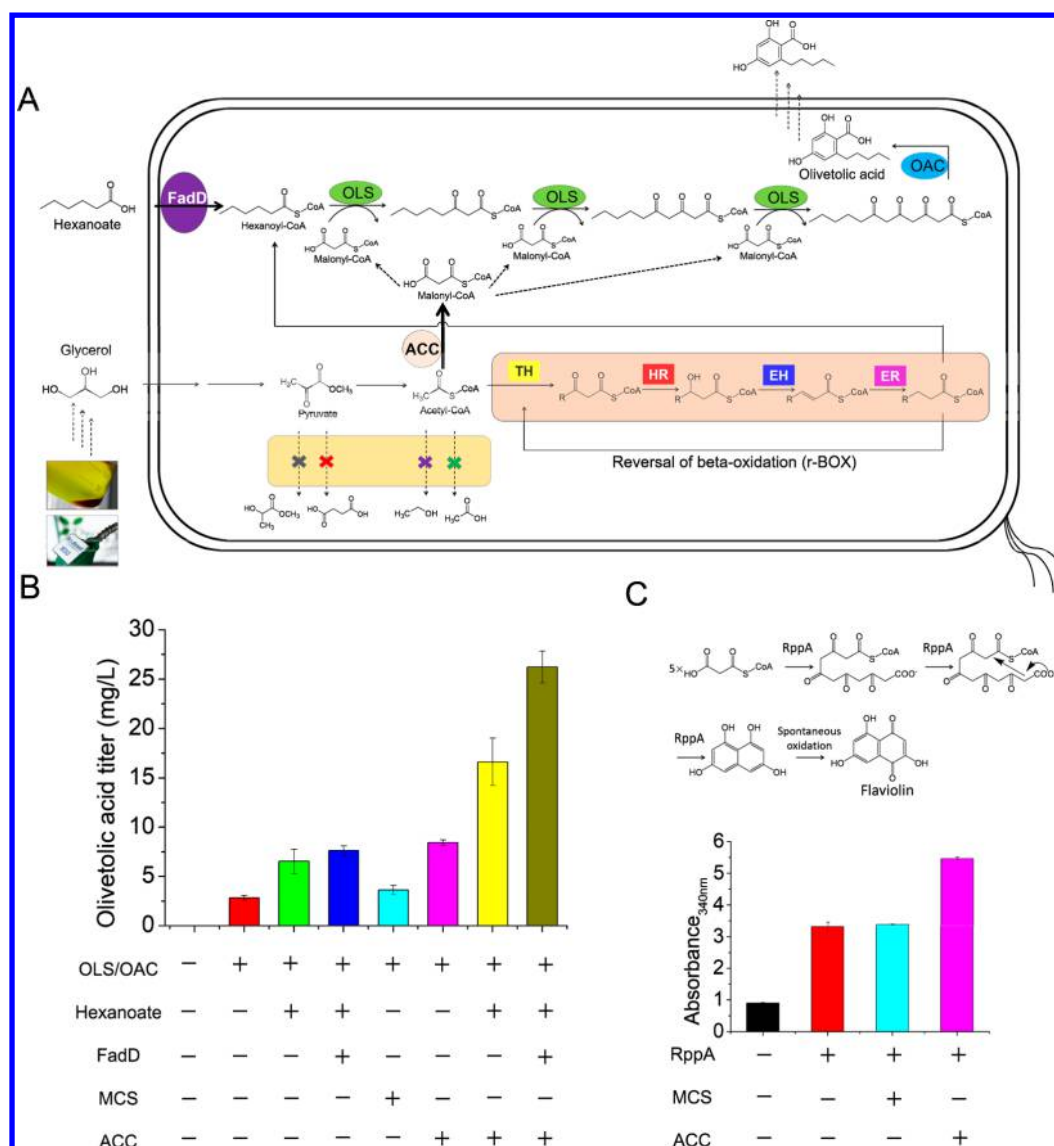


Figure 3. Production of olivetolic acid (OLA) in engineered *E. coli* JST10 (DE3). (A) In JST10 (DE3), a functional r-BOX was achieved by overexpression of BktB thiolase (TH), FadB hydroxyacyl-CoA dehydrogenase (HR), FadB enoyl-CoA hydratase (EH) and egTER enoyl-CoA reductase (ER). Fermentative byproduct (lactate, succinate, ethanol, acetate) pathways were blocked through deletion of *ldhA*, *frdA*, *adhE*, *pta*, and *poxB*. OLS-OAC core enzymes and FadD-ACC auxiliary enzymes were recruited for OLA production. (B) Olivetolic acid titers in different strains. Engineered *E. coli* strains were grown in LB-like MOPS medium + 2% (wt/v) glycerol supplemented with 4 mM hexanoate where indicated. For strains harboring MCS, 12 mM malonate sodium was also included. (C) Flaviolin biosynthesis pathway for measuring malonyl-CoA availability. Upper, flaviolin biosynthesis pathway: 5 malonyl-CoA are condensed by RppA to form flaviolin, which has a specific absorbance at wavelength of 340 nm. Bottom, RppA was expressed with different MCS/ACC auxiliary enzymes for characterization of malonyl-CoA availability in JST10 (DE3) strain. Engineered *E. coli* strains were cultured in LB-like MOPS medium + 2% (wt/v) glycerol. For strains harboring MCS, 12 mM malonate sodium was also included.

participating in the TCA cycle, glyoxylate cycle, amino acid metabolism, and other important pathways.²⁸ Although individual +ACC overexpression could channel more acetyl-CoA into malonyl-CoA available for OLA production, flux into other biosynthetic pathways and thus cellular growth may be impaired. Consistently, we observed lower growth with BL-OLS-OAC-ACC during the biotransformation (the highest OD₅₅₀ was only 1.8) compared with BL-OLS-OAC (the highest OD₅₅₀ was 3.8). Impaired growth caused by ACC overexpression has been observed in prior studies, in both *E. coli*²⁹ and *S. cerevisiae*.³⁰

While these initial experiments were conducted in the presence of hexanoate, the conversion of hexanoate to

hexanoyl-CoA in these strains may be inefficient due to potential low expression levels of *E. coli* native fatty acyl-CoA synthetase(s). To evaluate the impact of the hexanoyl-CoA pool on OLA production, two different *E. coli* native fatty acyl-CoA synthetases were overexpressed individually. FadK has been reported as an acyl-CoA synthetase which is primarily active on acetylation of short chain fatty acids (C6–C8).^{31,32} However, we found that overexpression of FadK had no impact on OLA production under these conditions (Figure 2). We also explored another native *E. coli* fatty acyl-CoA synthetase, FadD, which has broad chain length specificity, with maximal activities associated with fatty acids ranging in length from C12 to C18.^{33,34} Prior studies have showed that, compared to FadK,

despite the lower specificity for C6–C8, FadD exhibits a higher catalytic activity on C6–C8 fatty acids.³² The overexpression of FadD in combination with OLS and OAC (strain BL-OLS-OAC-FadD) resulted in slight increases in OLA titer (Figure 2). Combining this hexanoyl-CoA generating module with MCS, the highest OLA titer was achieved (0.71 mg/L) (Figure 2). However, FadD and MCS overexpression only resulted in a slight increase to OLA compared with MCS alone. Previous studies showed that different strains of *E. coli* show different production ability for different metabolites.^{35,36} In this regard, we tested the OLA production in BL21 (DE3) and *E. coli* K-12 MG1655 (DE3) strain, and found that MG1655 (DE3) gives similar OLA titers compared with BL21 (DE3) (Figure S3). Specifically, MG-OLS-OAC-FadD-MCS produced ~0.8 mg/L OLA (Figure S3), which is comparable to that in BL-OLS-OAC-FadD-MCS (0.71 mg/L). Overall, while these results demonstrate the importance of auxiliary enzymes for increasing malonyl-CoA and hexanoyl-CoA supply, the low OLA titers mandated us to investigate alternative approaches for further improving precursor supply.

Integration of the Synthetic Olivetolic Acid Pathway with a β -Oxidation Reversal for Precursor Supply. In contrast to the above approach, which relied on native metabolite pools or exogenous acid addition for malonyl-CoA and hexanoyl-CoA supply, an alternative to further improve OLA production involves the integrated engineering of pathways leading to precursor synthesis. With malonyl-CoA generated directly from acetyl-CoA, the availability of this intermediate may play a critical role in OLA production. Furthermore, the role of acetyl-CoA becomes even more important when considering potential routes for generating hexanoyl-CoA. In prior studies, both fatty acid biosynthesis (FAB) and β -oxidation reversal (r-BOX) pathways have been employed for the production of hexanoic acid.^{24,37,38} However, the FAB pathway operates with acyl carrier protein (ACP) intermediates that are directly converted to carboxylic acid products through the expression of heterologous specific short-chain C6-ACP thioesterase.^{38,39} For conversion of hexanoic acid to hexanoyl-CoA, expression of fatty acyl-CoA synthetase, such as FadD, is required. Furthermore, the FAB pathway also requires malonyl-CoA as the extender unit during elongation,⁴⁰ resulting in increased competition for malonyl-CoA. In contrast, r-BOX operates with CoA intermediates, utilizes acetyl-CoA as extender unit and can directly generate hexanoyl-CoA. With this pathway initiating from acetyl-CoA and requiring an additional 2 acetyl-CoA molecules to generate hexanoyl-CoA, ensuring high intracellular levels of this acetyl-CoA intermediate are critical.

To this end, we sought to exploit an engineered strain (JST10 (DE3)²⁴) which has been previously utilized for hexanoic acid synthesis through r-BOX. In addition to containing chromosomal expression constructs for the required thiolase (BktB), β -ketoacyl-CoA reductase (FadB), β -hydroxyacyl-CoA dehydratase (FadB), and trans-enoyl-CoA reductase (egTER) r-BOX modules, this *E. coli* MG1655 derivative has fermentative product pathways (e.g., lactate, succinate, acetate and ethanol) and thioesterases (e.g., *tesA* and *tesB* among others) deleted to ensure adequate acetyl-CoA supply and minimize the loss of acyl-CoA intermediates. As such, this strain is a promising background strain the expression of the synthetic OLA pathway (Figure 3A). Furthermore, the increased acetyl-CoA supply in this strain may also provide a means of utilizing ACC, opposed to MCS with exogenous malonate, for increasing malonyl-CoA availability.

Integration of r-BOX and the OLA biosynthesis pathway in JST10 (DE3) expressing OLS and OAC resulted in 2.8 mg/L OLA, nearly 30-fold higher than that in BL21 (DE3) (~0.1 mg/L), even in the absence of hexanoate addition (Figure 2). This result demonstrates the potential for OLA production from a single carbon source (glycerol) through utilizing r-BOX for generating hexanoyl-CoA. To evaluate if hexanoyl-CoA supply was still a limiting factor in this strain, we also conducted experiments in which 4 mM hexanoate was supplied. Under these conditions, JST10-OLS-OAC produced ~2.3-fold higher OLA (6.5 mg/L) indicating that improving hexanoyl-CoA availability could potentially increase OLA production. Interestingly, similar increases to OLA titer upon hexanoate supplementation was observed both with and without FadD expression under these conditions (Figure 3B).

We then assessed the impact of malonyl-CoA supply on OLA production through the overexpression of auxiliary enzymes. Although MCS was identified as the most effective malonyl-CoA supply strategy for OLA production in resting cells biotransformation experiments with BL21 (DE3) (Figure 2), in actively growing cultures of JST10 (DE3) the overexpression of ACC resulted in the highest increase in OLA titer (Figure 3B). Specifically, JST10-OLS-OAC-ACC produced 8.4 mg/L of olivetolic acid, 3-fold higher than JST10-OLS-OAC (2.8 mg/L) (p -value <0.05). JST10-OLS-OAC-MCS (with 12 mM malonate supplementation) produced 3.6 mg/L of olivetolic acid, which is a 28% increase compared to JST10-OLS-OAC (p -value <0.05) (Figure 3B). This is likely caused by two factors, both leading to higher levels of acetyl-CoA. First, the distinct metabolic backgrounds of BL21 (DE3) and JST10 (DE3), as the deletion of acetyl-CoA competitive and consumption pathways in JST10 (DE3) is likely to result in increased availability of acetyl-CoA for malonyl-CoA generation. Second, actively growing cultures of JST10 (DE3) should also lead to higher levels of acetyl-CoA (and higher production of malonyl-CoA upon ACC overexpression). To confirm increased malonyl-CoA supply in this background and conditions, a heterologous malonyl-CoA availability indicator pathway was introduced. Flaviolin biosynthesis requires a PKS III catalysis that uses malonyl-CoA as both primer and extender unit.⁴¹ Specifically, the polyketide synthase RppA⁴¹ from *Streptomyces griseus*, which iteratively condenses 5 molecules of malonyl-CoA to form flaviolin (which has a specific absorbance at the wavelength of 340 nm), was introduced into JST10 (DE3) strains (Figure 3C). While no significant increase in A₃₄₀ was observed upon the combined overexpression of RppA and MCS (with 12 mM malonate supplementation) compared to RppA only, the overexpression of ACC with RppA lead to a significant increase in absorbance (Figure 3D) (p -value <0.05). These results provide further evidence that ACC overexpression is an effective strategy to increase malonyl-CoA supply in JST10 (DE3), which in turn leads to higher OLA production.

Given the impact of auxiliary enzymes and individually increasing hexanoyl-CoA and malonyl-CoA supply in JST10 (DE3), we next evaluated their combination in conjunction with the synthetic OLA pathway. As seen in Figure 3B, additional hexanoate supplementation during fermentation with JST10-OLS-OAC-ACC resulted in a 2-fold increase in OLA titer to 16.6 mg/L (p -value <0.05) (Figure 3B). Moreover, despite the overexpression of FadD having a negligible impact with hexanoate feeding and OLS/OAC overexpression, combined with ACC overexpression FadD significantly improved OLA titer (26.2 mg/L) (Figure 3B). This indicates the importance of

both hexanoyl-CoA and malonyl-CoA supply, as either can become the limiting factor as intracellular supply of each is increased. We also evaluated the dosage effect of hexanoate supplementation on OLA production and found that feeding 4 mM hexanoate contributes to the highest titer of OLA (Figure S4). As such, coordinated increase in the supply of hexanoyl-CoA and malonyl-CoA is critical for producing OLA at high levels. While external addition to hexanoate was required here to increase titers, we also demonstrate a new application of r-BOX. Although prior studies of engineering of r-BOX primarily focused on production of short-chain fatty acids or alcohols,^{23,24,42} here we demonstrated that this pathway can also be employed to supply the starting CoA primer for polyketide biosynthesis.

Optimization of Fermentation Conditions for Olivetolic Acid Production. Following the establishment of the best combination of enzymatic components for OLA production, we attempted to optimize the fermentation conditions for further titer improvement with strain JST10-OLS-OAC-FadD-ACC. This included evaluation of the impact of various temperatures, working volumes, and inducer concentrations on OLA production (Figure 4). Results showed that 37 °C (26.8 mg/

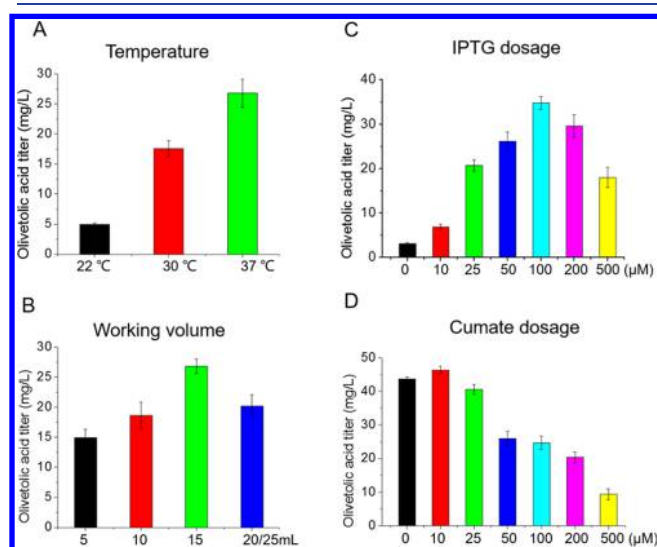


Figure 4. Optimization of fermentation conditions for olivetolic acid production by JST10-OLS-OAC-FadD-ACC. The engineered *E. coli* strain was cultured in LB-like MOPS medium + 2% (wt/v) glycerol in 25 mL shake flasks. (A) Effects of different temperature on OLA production with gene expression induced by 50 μM IPTG and 100 μM cumate. (B) Effects of different working volume (WV) on OLA production with gene expression induced by 50 μM IPTG and 100 μM cumate. (C) Effects of different IPTG dosages on OLA production with 100 μM cumate. (D) Effects of different cumate dosage on OLA production with 100 μM IPTG. For all experiments, inducers and 4 mM hexanoate were added after strains reached an $OD_{550} \sim 0.4$ – 0.8 .

L) was the optimal temperature for OLA production with a significant decrease in titer at both 30 °C (17.6 mg/L) and 22 °C (5.0 mg/L) (Figure 4A). Based on the identified optimal temperature (37 °C), we further studied the impact of working volume (WV, X mL in 25 mL flask, X/25 mL) as a means of altering aeration. We found that the engineered strain had the highest OLA titer of 26.8 mg/L at a WV of 15/25 mL (Figure 4B). In addition to temperature and WV, we further investigated the impact of inducer concentrations (IPTG and cumate) on OLA production. In the engineered strain, genes encoding OLS,

OAC, FadD, and ACC enzymes are expressed under the control of inducible T7 promoter, for which IPTG serves as inducer. Excessive IPTG addition has been reported to be toxic to *E. coli* cells and will cause inclusion body formation for excessive proteins biosynthesis,⁴³ resulting in inhibition of enzymatic activities and thus decreased product biosynthesis.⁴⁴ To this end, optimization of IPTG dosage for OLA production is desirable. Results showed that the JST10-OLS-OAC-FadD-ACC strain still produced 3.1 mg/L of OLA without addition of IPTG, likely due to leaky expression under the T7 promoter (Figure 4C). Upon induction by IPTG, OLA production increased significantly and a positive correlation was observed between IPTG dosage and OLA titer up to 100 μM. With 100 μM IPTG, the JST10-OLS-OAC-FadD-ACC strain produced 34.8 mg/L of OLA (Figure 4C), which is 30% higher the best titers achieved by using 50 μM IPTG. However, excessive dosage of IPTG (>100 μM) was found to decrease OLA production.

We also optimized the dosage effect of the inducer cumate, which activates the expression of enzymes in r-BOX by binding with CymR repressor.⁴⁵ Results showed that, the JST10-OLS-OAC-FadD-ACC strain produced the highest level of OLA at 46.3 mg/L when cumate was added at 10 μM (Figure 4D). It is not surprising that the optimal dosage of cumate inducer is relatively lower than optimal IPTG inducer (100 μM) since cumate-inducible r-BOX genes, *i.e.*, *bktB*, *fadB*, *egTER*, were integrated at the single site (*atoB*, *fadB* and *fabI* loci, respectively)³⁷ of chromosomal DNA of JST10 (DE3) instead of plasmids, and thus a small dosage of cumate should be enough for switching on the expression of these genes. Similar to IPTG, excessive cumate dosage also compromised OLA production (Figure 4D).

Olivetolic Acid Fermentation in Bioreactor under Controlled Conditions. In order to obtain higher OLA titer, a batch fermentation with precise parameter control was conducted using the engineered strain JST10-OLS-OAC-FadD-ACC and the identified optimal fermentation conditions. Under these conditions, cell growth of JST10-OLS-OAC-FadD-ACC reached the highest OD_{550} of 8 (corresponding cell mass is approximately 2.64 g/L) at 48 h. During the first 24 h, JST10-OLS-OAC-FadD-ACC consumed a total of ~8.5 g/L of glycerol, 79 mg/L of hexanoate and produced approximately 80 mg/L of OLA (Figure 5A). To our knowledge, this is the highest OLA titer achieved in any wild type or engineered microorganism. In addition, moderate accumulation of pyruvate was observed in the fermentation medium for removal of downstream byproducts pathways (Figure 3A). Also, although *pta* was deleted in JST10, a small amount of acetate still produced, which might be due to presence of other unknown endogenous transferase within *E. coli* (Figure S5). Formation of both unwanted byproducts compromised the OLA yield. Further, we continued to analyze the toxicity of OLA to *E. coli*, and revealed that up to 100 mg/L of OLA did not impact the final cell mass of *E. coli* (Figure S6), which excluded the possibility that the product toxicity compromised OLA production.

Furthermore, we also observed that with the increase of fermentation time, OLA titer decreased. Specifically, from 24 to 48 h OLA concentration decreased by 50% to 37.4 mg/L. We hypothesize that the observed decrease in OLA concentration could be due to (1) OLA is inherently unstable and will degrade spontaneously in aqueous environments; (2) OLA can be metabolized by *E. coli* cells. We further analyzed the stability of

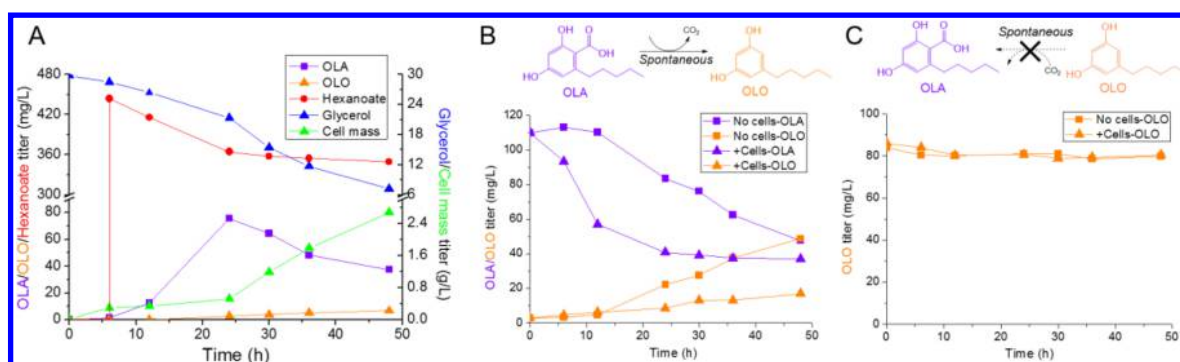


Figure 5. Olivetolic acid (OLA) production and stability. (A) OLA fermentation in bioreactor with controlled conditions. Fermentation was performed in 400 mL MOPS medium with 30 g/L glycerol in 500 mL bioreactor (Infors). Cultures were grown at 37 °C with an initial OD_{550} of 0.07, 100 μ M IPTG, 10 μ M cumate and 4 mM hexanoate were added when OD_{550} reached 0.4–0.8, the pH was maintained at 7.0 by using 1.5 M H_2SO_4 and 3 M NaOH, the dissolved oxygen level was also monitored. (B) Olivetolic acid stability assays in the absence/presence of *E. coli* MG1655 (DE3) cells. The initial olivetolic acid titer was \sim 110 mg/L. (C) Olivetol stability assay in the absence/presence of *E. coli* MG1655 (DE3) cells. All the olivetolic acid/olivetol stability assays were conducted in 400 mL MOPS medium with 30 g/L glycerol in 500 mL Infors bioreactor. In the presence of *E. coli* cells, *E. coli* initial inoculum was set as $OD_{550} \sim$ 0.07. OLA, olivetolic acid; OLO, olivetol.

OLA in the absence and presence of wild type *E. coli* cells (Figure 5B) and determined that even in the absence of *E. coli* MG1655 (DE3), OLA levels decreased over time, with the majority of OLA decarboxylated to olivetol (Figure 5B). In the presence of *E. coli* cells, although a portion was still observed to form olivetol, OLA was degraded more than in the absence of cells, indicating at least a fraction of OLA was metabolized by *E. coli* (Figure 5B). Conversely, to further determine whether olivetol can spontaneously convert to OLA or be metabolized by *E. coli* cells, we conducted a similar experiments with olivetol. Results showed that olivetol can neither spontaneously convert to OLA nor be metabolized by *E. coli* cells under our experimental conditions (Figure 5B). Olivetol seems more stable than OLA in aqueous environments, which might be related to the absence of a carboxyl group.⁴⁶

CONCLUSIONS

Despite the structural complexity of plant polyketides, the tractable starting units required for their synthesis enables a synthetic approach for their production in which PKS and cyclase components can be integrated with pathways for the generation of primer and extender units. Here, functional expression and characterization of the *Cannabis sativa* OLA synthase and cyclase enzymes confirmed their requirement for the synthesis of OLA from hexanoyl-CoA and malonyl-CoA. Through the direct integration of OLS and OAC with modules of the β -oxidation reversal aimed at generating hexanoyl-CoA, we demonstrate the synthesis of the plant natural product OLA in engineered *E. coli* from a single carbon source. By further combining these pathways with auxiliary enzymes for additional hexanoyl-CoA and malonyl-CoA generation, we also identified the supply of these precursors as a key limiting factor in OLA synthesis. Through combinational utilization of these auxiliary enzymes and optimization of fermentation conditions, we achieved an OLA titer of \sim 80 mg/L. This represents the first report of OLA synthesis in *E. coli*, and further demonstrates the potential for microbial cell factories to overcome the limitations of direct plant extraction or chemical synthesis to produce plant-based natural products.

METHODS

Strains and Culture Conditions. All strains used in this study are listed in Table 1. *E. coli* BL21 (DE3) and JST10 (DE3)

were employed as the host strains. Luria–Bertani (LB) medium was used for culturing *E. coli* cells for plasmid construction. Modified M9Y medium (6.7 g/L Na_2HPO_4 , 3 g/L KH_2PO_4 , 0.5 g/L NaCl, 1 g/L of NH_4Cl , 20 g/L glucose, 10 g/L yeast extract, 2 mM $MgSO_4$, and 0.1 mM $CaCl_2$) was used for the resting cells biotransformation experiments with all BL21 (DE3) derivatives strains.^{24,42,47} The “LB-like” MOPS medium used for JST10 (DE3) strains contains 125 mM MOPS, supplemented with 20 g/L glycerol (or 30 g/L in batch fermentation and olivetolic acid/olivetol stability assays), 10 g/L tryptone, 5 g/L yeast extract, 5 mM calcium pantothenate, 2.78 mM Na_2HPO_4 , 5 mM $(NH_4)_2SO_4$, 30 mM NH_4Cl , 5 μ M sodium selenite, 100 μ M $FeSO_4$.²⁴ When necessary, ampicillin, spectinomycin and kanamycin were added at final concentrations of 100, 50, and 50 mg/L, respectively.

Construction of Plasmids. All oligonucleotide primers used in this study are listed in Table S1. Codon optimized OLS and OAC^{17,18} from *Cannabis sativa* for expression in *E. coli* were synthesized by GeneArt (Invitrogen) and then inserted into the first and second multiple cloning site of pETDuet-1, respectively, resulting into pET-P1-OLS-P2-OAC. FadD and FadK were PCR-amplified from *E. coli* K-12 MG1655 genomic DNA and inserted into the first cloning site of pCDFDuet-1 to obtain pCDF-P1-FadD/FadK. The malonyl-CoA synthetase (MCS) gene from *Bradyrhizobium japonicum*²⁷ was codon optimized and inserted into the second multiple cloning site of pCDFDuet-1 to obtain pCDF-P2-MCS. AccA, AccB, AccC and AccD were PCR-amplified from MG1655 genomic DNA with a ribosome binding site (RBS) (underlined, Table S1) and assembled into the second multiple cloning site of pCDFDuet-1 through Gibson Assembly Cloning Kit (NEB) to obtain pCDF-P2-ACC.

In Vitro Production of Olivetolic Acid. *E. coli* BL21 (DE3) was used for expression of His-tagged OLS and OAC proteins, from their respective pET-P1-OLS and pET-P1-OAC constructs. BL21 (DE3) strains containing His-tagged OAC or OLS genes were grown at 37 °C in 0.5 L LB medium with ampicillin. Enzyme expression was induced by addition of isopropyl- β -D-thiogalactoside (IPTG) to a final concentration of 0.4 mM, when OD_{550} of the culture was between 0.4 and 0.8. After 18 h of induction at 37 °C, cells were harvested by centrifugation at 12 000 rpm, 4 °C, 10 min. The cell pellet was resuspended in lysis buffer (20 mM Tris-HCl, 0.5 M NaCl, 5 mM imidazole,

Table 1. Strains and Plasmids Used in This Study

plasmids/strains	genetic characteristics	source
Plasmids		
pETDuet-1	pBR322 ori with P _{T7} ; Amp ^R	Novagen
pCDFDuet-1	CDF ori with P _{T7} ; Sm ^R	Novagen
pET-P1-OLS	pETDuet-1 carrying <i>ols</i>	This study
pET-P1-OAC	pETDuet-1 carrying <i>oac</i>	This study
pET-P1-OLS-P2-OAC	pETDuet-1 carrying <i>ols</i> and <i>oac</i>	This study
pCDF-P1-FadD	pCDFDuet-1 carrying <i>fadD</i>	This study
pCDF-P1-FadK	pCDFDuet-1 carrying <i>fadK</i>	This study
pCDF-P2-MCS	pCDFDuet-1 carrying <i>mcs</i>	This study
pCDF-P2-ACC	pCDFDuet-1 carrying <i>accA</i> , <i>accB</i> , <i>accC</i> , <i>accD</i>	This study
pCDF-P1-FadD-P2-MCS	pCDFDuet-1 carrying <i>fadD</i> and <i>mcs</i>	This study
pCDF-P1-FadK-P2-MCS	pCDFDuet-1 carrying <i>fadK</i> and <i>mcs</i>	This study
pCDF-P1-FadD-P2-ACC	pCDFDuet-1 carrying <i>fadD</i> and <i>accA</i> , <i>accB</i> , <i>accC</i> , <i>accD</i>	This study
pCDF-P1-FadK-P2-ACC	pCDFDuet-1 carrying <i>fadK</i> and <i>accA</i> , <i>accB</i> , <i>accC</i> , <i>accD</i>	This study
pET-P1-RppA	pETDuet-1 carrying <i>rppA</i>	This study
<i>E. coli</i> Strains		
<i>E. coli</i> BL21 (DE3)	Host strain for enzymes expression	Lab collection
<i>E. coli</i> JST10 (DE3)	$\Delta frdA \Delta ldhA \Delta pta \Delta adhE \Delta poxB \Delta yciA \Delta ybgC \Delta ydiI \Delta tesA \Delta fadM \Delta tesB \Delta fadE$ DE3 FRT- <i>cymR</i> -P ^{CT5} - <i>fadB</i> $\Delta fadA::zeo$ FRT- <i>cymR</i> -P ^{CT5} - <i>bktB</i> $\Delta atoB$ FRT- <i>cymR</i> -P ^{CT5} - <i>egT_{ER}</i> at <i>fabI</i> chromosomal location	24
BL-OLS-OAC	BL21 (DE3) with pET-P1-OLS-P2-OAC	This study
BL-OLS-OAC-FadD	BL21 (DE3) with pET-P1-OLS-P2-OAC and pCDF-P1-FadD	This study
BL-OLS-OAC-FadK	BL21 (DE3) with pET-P1-OLS-P2-OAC and pCDF-P1-FadK	This study
BL-OLS-OAC-MCS	BL21 (DE3) with pET-P1-OLS-P2-OAC and pCDF-P2-MCS	This study
BL-OLS-OAC-ACC	BL21 (DE3) with pET-P1-OLS-P2-OAC and pCDF-P1-ACC	This study
BL-OLS-OAC-FadD-MCS	BL21 (DE3) with pET-P1-OLS-P2-OAC and pCDF-P1-FadD-P2-MCS	This study
BL-OLS-OAC-FadK-MCS	BL21 (DE3) with pET-P1-OLS-P2-OAC and pCDF-P1-FadK-P2-MCS	This study
BL-OLS-OAC-FadD-ACC	BL21 (DE3) with pET-P1-OLS-P2-OAC and pCDF-P1-FadD-P2-ACC	This study
BL-OLS-OAC-FadK-ACC	BL21 (DE3) with pET-P1-OLS-P2-OAC and pCDF-P1-FadK-P2-ACC	This study
MG-OLS-OAC	MG1655 (DE3) with pET-P1-OLS-P2-OAC	This study
MG-OLS-OAC-FadD-MCS	MG1655 (DE3) with pET-P1-OLS-P2-OAC and pCDF-P1-FadD-P2-MCS	This study
MG-OLS-OAC-FadD-ACC	MG1655 (DE3) with pET-P1-OLS-P2-OAC and pCDF-P1-FadD-P2-ACC	This study
JST10-OLS-OAC	JST10 (DE3) with pET-P1-OLS-P2-OAC	This study
JST10-OLS-OAC-FadD-MCS	JST10 (DE3) with pET-P1-OLS-P2-OAC and pCDF-P1-FadD-P2-MCS	This study
JST10-OLS-OAC-FadD-ACC	JST10 (DE3) with pET-P1-OLS-P2-OAC and pCDF-P1-FadD-P2-ACC	This study
JST10-OLS-OAC-FadD	JST10 (DE3) with pET-P1-OLS-P2-OAC and pCDF-P1-FadD	This study
JST10-OLS-OAC-ACC	JST10 (DE3) with pET-P1-OLS-P2-OAC and pCDF-P2-ACC	This study
JST10-OLS-OAC-MCS	JST10 (DE3) with pET-P1-OLS-P2-OAC and pCDF-P2-MCS	This study
JST10-RppA	JST10 (DE3) with pET-P1-RppA	This study
JST10-MCS-RppA	JST10 (DE3) with pET-P1-RppA and pCDF-P2-MCS	This study
JST10-ACC-RppA	JST10 (DE3) with pET-P1-RppA and pCDF-P2-ACC	This study

0.1% Triton-X 100, pH 8.0) and subjected to sonication using a Sonifier SFX250 (Branson). Following centrifugation (10 000 rpm, 4 °C, 30 min), the supernatant containing soluble protein fraction was recovered and filtered through a 0.45 μm filter.

Recombinant His-tagged proteins were purified using TALON metal affinity resin (Clontech). Soluble protein extract was applied to 1 mL packed column of the resin, and after washing the unbound proteins with wash buffer (20 mM Tris-HCl, 0.5 M

NaCl, pH 8.0) supplemented with 20 mM imidazole, the His-tagged enzymes were eluted from the column with elution buffer containing 250 mM imidazole. Purified His-tagged enzymes were concentrated to a final concentration of 2 mg/mL and elution buffer was exchanged with storage buffer (12.5 mM Tris-HCl, 50 mM NaCl and 2 mM DTT) at 4 °C using Amicon ultrafiltration centrifugal devices. The concentrated enzymes were stored at -80 °C for enzyme activity assays. Enzyme assays were performed in a 500 μ L total reaction volume containing 100 mM potassium phosphate buffer (pH 7.0), 200 μ M hexanoyl-CoA, 400 μ M malonyl-CoA, 10 μ g OLS, and 30 μ g OAC (when included).¹⁸ The reaction mixture was incubated at 20 °C for 16 h and 20 μ L sulfuric acid (H₂SO₄) was added to terminate the reaction.

Resting Cell Biotransformations for Olivetolic Acid Production. One milliliter (1 mL) of overnight cultures of recombinant *E. coli* strains was inoculated in 50 mL fresh LB medium in 250 mL shake flask with ampicillin, and cultivated at 37 °C, 200 rpm. When OD₅₅₀ reached approximately 0.4–0.8, 0.5 mM IPTG was added. The cultures were then incubated at 22 °C for 15 h. Cells were then harvested by centrifugation, washed with fresh M9Y medium and resuspended in 50 mL M9Y medium to OD₅₅₀ \sim 3 and supplied with 4 mM hexanoate for biotransformation experiments.^{15,48,49} An additional 12 mM sodium malonate was added when malonyl-CoA synthetase (MCS) was expressed for malonyl-CoA synthesis. Following incubation at 22 °C for 48 h, the fermentation broth supernatants were extracted by equal volume of ethyl acetate, evaporated by nitrogen and resuspended in 1 mL methanol for HPLC-MS analysis by using Agilent 1200 HPLC system and Bruker MicroToF ESI LC-MS System. The column used was Shim-pack XR-ODS II C18, 2.0 mm \times 75 mm (Shimadzu). HPLC conditions were as follows: solvent A = 0.1% formic acid in H₂O; solvent B = methanol; flow rate = 0.25 mL min⁻¹; 0–2.5 min, 95% A and 5% B; 2.5–20 min, 95% A and 5% B to 5% A and 95% B; 20–23 min, 5% A and 95% B; 23–24 min, 5% A and 95% B to 95% A and 5% B; 24–30 min, 95% A and 5% B.^{15,48,49}

Fermentation Conditions for Olivetolic Acid Production in Shake Flasks. Modified LB-like MOPS medium using glycerol as carbon source was used for all fermentations.²⁴ Fermentations were conducted in 25 mL Pyrex Erlenmeyer flasks (narrow mouth/heavy duty rim, Corning) filled with 5–20 mL of the MOPS medium with 20 g/L glycerol and sealed with foam plugs filling the necks.²⁴ A single colony of the desired strain was cultivated overnight (14–16 h) in LB medium with appropriate antibiotics and used as the initial inoculum at the OD₅₅₀ \sim 0.07. After inoculation, flasks were incubated at 37 °C and 200 rpm until OD₅₅₀ reached 0.4–0.8, at which point IPTG (0–500 μ M), cumate (0–500 μ M) and hexanoate (4 mM) were added. Twelve mM sodium malonate was also added when malonyl-CoA synthetase (MCS) was expressed for malonyl-CoA synthesis. Flasks were then incubated under the same conditions for 48 h postinduction unless otherwise stated.

Olivetolic Acid Fermentation in Bioreactor with Precise Parameter Control. Fermentations were performed in 400 mL MOPS medium with 30 g/L glycerol in a 500 mL bioreactor (Infors) at 37 °C. An overnight seed culture was used to inoculate the bioreactor to an of OD₅₅₀ \sim 0.07 and when the OD₅₅₀ reached 0.4–0.8, 100 μ M IPTG, 10 μ M cumate and 4 mM hexanoate were added. pH was maintained at 7.0 by using 1.5 M sulfuric acid (H₂SO₄) as acid solution and 3 M potassium hydroxide (NaOH) as base solution. The air flow rate was set at 50 mL/min, stirring speed was set at 720 rpm. The dissolved

oxygen (DO) level was set at 100% at the beginning, with DO level monitored but not controlled during the whole fermentation period.

Olivetolic Acid/Olivetol Stability Analysis. For olivetolic acid stability assays, 500 bioreactors with the above-described media and conditions were utilized. The initial olivetolic acid concentration was \sim 110 mg/L for olivetolic acid stability analysis. In the presence of *E. coli* cells, MG1655 (DE3) was employed as the testing strain. An overnight seed culture was used to inoculate the bioreactor an OD₅₅₀ \sim 0.07. pH was maintained at 7.0 by using 1.5 M H₂SO₄ and 3 M NaOH. The air flow rate was set at 50 mL/min.

Similar operation was performed for olivetol stability assay, only changing the initial olivetolic acid to olivetol (\sim 80 mg/L).

GC-FID/MS Analysis. Quantification of olivetolic acid was conducted via GC-FID analysis using an Agilent 7890 B gas chromatograph equipped with an Agilent 5977 mass spectroscope detector (Agilent) and an HP-5 ms capillary column (0.25 mm internal diameter, 0.25 μ m film thickness, 30 m length; Agilent). Sample preparation was conducted as follows:⁵⁰ 2 mL culture samples were transferred to 5 mL glass vials (Fisher Scientific), 4-pentylbenzoic acid (final concentration 50 mg/L) was added as internal standard. Then 80 μ L of H₂SO₄ and 340 μ L of 30% (wt/v) NaCl solution were added for pH and ionic strength adjustment. Two milliliters of hexane was added for extraction. Vials were sealed with Teflon-lined septa (Fisher Scientific), secured with caps, and rotated at 60 rpm for 2 h. The samples were then centrifuged for 2 min at 6500 rpm to separate the aqueous and organic layers. After centrifugation, 1.5 mL of the top organic layer was transferred to new 5 mL glass vial and evaporated under a stream of nitrogen. Then, 100 μ L pyridine and 100 μ L of *N,O*-Bis(trimethylsilyl)trifluoroacetamide (BSTFA) were added to the dried extract for derivatization at 70 °C for 1 h. After cooling to room temperature, 200 μ L of derivatization product was transferred to vials (Fisher Scientific) for GC-MS analysis according to the following method: 1 μ L were injected into the GC, which was run in splitless mode using helium gas as a carrier gas with a flow rate of 1 mL/min. The injector temperature was 280 °C and the oven temperature was initially held at 50 °C for 3 min and then raised to 250 °C at 10 °C/min and held for 3 min.

Statistical Analysis. The two-tailed *t*-test method was employed to analyze the statistical significance of all data in this study and *p*-value <0.05 is deemed statistically significant.

■ ASSOCIATED CONTENT

📄 Supporting Information

The Supporting Information is available free of charge on the ACS Publications website at DOI: [10.1021/acssynbio.8b00075](https://doi.org/10.1021/acssynbio.8b00075).

Table S1: Primers used in this study; Figure S1: Expression of OLS and OAC in BL21 (DE3); Figure S2: Mass spectrometry results of olivetolic acid, olivetol and PDAL by using GC-MS; Figure S3: Comparison of BL21 (DE3) with MG1655 (DE3) for olivetolic acid production; Figure S4: Effect of fed hexanoate dosage on olivetolic acid production; Figure S5: Byproducts formation during olivetolic acid (OLA) production; Figure S6: Toxicity of olivetolic acid (OLA) to *E. coli* (PDF)

AUTHOR INFORMATION

Corresponding Author

*Phone: (713) 348-4893. Fax: (713) 348-5478. E-mail: ramon.gonzalez@rice.edu.

ORCID

Ramon Gonzalez: 0000-0003-4797-6580

Author Contributions

R.G. designed research; Z.T. and J.M.C. performed research; Z.T. and J.M.C. analyzed data; Z.T., J.M.C., and R.G. wrote the paper.

Notes

The authors declare the following competing financial interest(s): R.G. owns shares in Bioactive Ingredients Corporation.

ACKNOWLEDGMENTS

This work was supported by Bioactive Ingredients Corporation. The funders had no role in study design, data collection and analysis, decision to publish, or preparation of the manuscript. The authors thank Seokjung Cheong for assistance with gene cloning, Shivani Garg for help with enzyme purification, and Seohyoung Kim for assistance with bioreactor fermentations.

ABBREVIATIONS

OLA, olivetolic acid; OLO, olivetol; PDAL, pentyl diacetic acid lactone; HTAL, hexanoyl triacetic acid lactone; FadD, long chain fatty acid CoA-ligase; FadK, short chain acyl-CoA synthetase; ACC, acetyl-CoA carboxylase; MCS, malonyl-CoA synthetase; r-BOX, reversal of β -oxidation; IPTG, isopropyl- β -D-thiogalactopyranoside; BSTFA, *N,O*-Bis(trimethylsilyl)-trifluoroacetamide.

REFERENCES

- (1) Zhou, W., Zhuang, Y., Bai, Y., Bi, H., Liu, T., and Ma, Y. (2016) Biosynthesis of phlorisovalerophenone and 4-hydroxy-6-isobutyl-2-pyrone in *Escherichia coli* from glucose. *Microb. Cell Fact.* 15, 149.
- (2) Yu, D. Y., Xu, F. C., Zeng, J., and Zhan, J. X. (2012) Type III polyketide synthases in natural product biosynthesis. *IUBMB Life* 64, 285–295.
- (3) Li, H., Liang, J., Chen, H., Ding, G., Ma, B., and He, N. (2016) Evolutionary and functional analysis of mulberry type III polyketide synthases. *BMC Genomics* 17, 540.
- (4) Ismed, F., Farhan, A., Bakhtiar, A., Zaini, F., Nugraha, Y. P., Putra, O. D., and Uckusa, H. (2016) Crystal structure of olivetolic acid: a natural product from *Cetrelia sanguinea* (Schaer. *Acta Crystallogr. E* 72, 1587–1589.
- (5) Costain, W. J., Tauskela, J. S., Rasquinha, I., Comas, T., Hewitt, M., Marleau, V., and Soo, E. C. (2016) Pharmacological characterization of emerging synthetic cannabinoids in HEK293T cells and hippocampal neurons. *Eur. J. Pharmacol.* 786, 234–245.
- (6) Tai, S., and Fantegrossi, W. E. (2014) Synthetic Cannabinoids: Pharmacology, Behavioral Effects, and Abuse Potential. *Current addiction reports*. 1, 129–136.
- (7) Huestis, M. A. (2007) Human cannabinoid pharmacokinetics. *Chem. Biodiversity* 4, 1770–1804.
- (8) Andre, C. M., Hausman, J. F., and Guerriero, G. (2016) Cannabis sativa: The Plant of the Thousand and One Molecules. *Front. Plant Sci.*, DOI: 10.3389/fpls.2016.00019.
- (9) Hazekamp, A., Simons, R., Peltenburg-Looman, A., Sengers, M., van Zweden, R., and Verpoorte, R. (2004) Preparative isolation of cannabinoids from *Cannabis sativa* by centrifugal partition chromatography. *J. Liq. Chromatogr. Relat. Technol.* 27, 2421–2439.
- (10) Yoshimatsu, K., Iida, O., Kitazawa, T., Sekine, T., Kojoma, M., Makino, Y., and Kiuchi, F. (2004) Growth characteristics of *Cannabis sativa* L. cultivated in a phytotron and in the field. *Kokuritsu Iyakuhin Shokuhin Eisei Kenkyujo Hokoku*, 16–20.
- (11) Yao, J., Weng, Y. Q., Dickey, A., and Wang, K. Y. (2015) Plants as Factories for Human Pharmaceuticals: Applications and Challenges. *Int. J. Mol. Sci.* 16, 28549–28565.
- (12) Chittiboyina, A., and Khan, I. (2012) Short synthesis of olivetolic acid via Directed ortho-Metalation (DoM). *Planta Med.* 78, 42.
- (13) Liu, X., Ding, W., and Jiang, H. (2017) Engineering microbial cell factories for the production of plant natural products: from design principles to industrial-scale production. *Microb. Cell Fact.* 16, 125.
- (14) Ajikumar, P. K., Xiao, W. H., Tyo, K. E., Wang, Y., Simeon, F., Leonard, E., Mucha, O., Phon, T. H., Pfeifer, B., and Stephanopoulos, G. (2010) Isoprenoid pathway optimization for Taxol precursor overproduction in *Escherichia coli*. *Science* 330, 70–74.
- (15) Bai, Y., Yin, H., Bi, H., Zhuang, Y., Liu, T., and Ma, Y. (2016) De novo biosynthesis of Gastrodin in *Escherichia coli*. *Metab. Eng.* 35, 138–147.
- (16) Ro, D. K., Paradise, E. M., Ouellet, M., Fisher, K. J., Newman, K. L., Ndungu, J. M., Ho, K. A., Eachus, R. A., Ham, T. S., Kirby, J., Chang, M. C., Withers, S. T., Shiba, Y., Sarpong, R., and Keasling, J. D. (2006) Production of the antimalarial drug precursor artemisinic acid in engineered yeast. *Nature* 440, 940–943.
- (17) Taura, F., Tanaka, S., Taguchi, C., Fukamizu, T., Tanaka, H., Shoyama, Y., and Morimoto, S. (2009) Characterization of olivetol synthase, a polyketide synthase putatively involved in cannabinoid biosynthetic pathway. *FEBS Lett.* 583, 2061–2066.
- (18) Gagne, S. J., Stout, J. M., Liu, E., Boubakir, Z., Clark, S. M., and Page, J. E. (2012) Identification of olivetolic acid cyclase from *Cannabis sativa* reveals a unique catalytic route to plant polyketides. *Proc. Natl. Acad. Sci. U. S. A.* 109, 12811–12816.
- (19) Krivoruchko, A., Zhang, Y., Siewers, V., Chen, Y., and Nielsen, J. (2015) Microbial acetyl-CoA metabolism and metabolic engineering. *Metab. Eng.* 28, 28–42.
- (20) Vadali, R. V., Horton, C. E., Rudolph, F. B., Bennett, G. N., and San, K. Y. (2004) Production of isoamyl acetate in *ackA-pta* and/or *ldh* mutants of *Escherichia coli* with overexpression of yeast ATF2. *Appl. Microbiol. Biotechnol.* 63, 698–704.
- (21) Lin, F., Chen, Y., Levine, R., Lee, K., Yuan, Y., and Lin, X. N. (2013) Improving fatty acid availability for bio-hydrocarbon production in *Escherichia coli* by metabolic engineering. *PLoS One* 8, e78595.
- (22) Zhou, S., Iverson, A. G., and Grayburn, W. S. (2008) Engineering a native homoethanol pathway in *Escherichia coli* B for ethanol production. *Biotechnol. Lett.* 30, 335–342.
- (23) Dellomonaco, C., Clomburg, J. M., Miller, E. N., and Gonzalez, R. (2011) Engineered reversal of the beta-oxidation cycle for the synthesis of fuels and chemicals. *Nature* 476, 355–359.
- (24) Kim, S., Clomburg, J. M., and Gonzalez, R. (2015) Synthesis of medium-chain length (C6-C10) fuels and chemicals via beta-oxidation reversal in *Escherichia coli*. *J. Ind. Microbiol. Biotechnol.* 42, 465–475.
- (25) Yang, J., Xiong, Z. Q., Song, S. J., Wang, J. F., Lv, H. J., and Wang, Y. (2015) Improving heterologous polyketide production in *Escherichia coli* by transporter engineering. *Appl. Microbiol. Biotechnol.* 99, 8691–8700.
- (26) Kim, Y. S., and Bang, S. K. (1985) Malonyl coenzyme A synthetase. Purification and properties. *J. Biol. Chem.* 260, 5098–5104.
- (27) Kim, Y. S., and Kang, S. W. (1994) Steady-state kinetics of malonyl-CoA synthetase from *Bradyrhizobium japonicum* and evidence for Malonyl-AMP formation in the reaction. *Biochem. J.* 297, 327–333.
- (28) Wolfe, A. J. (2005) The acetate switch. *Microbiology and molecular biology reviews: MMBR.* 69, 12–50.
- (29) Davis, M. S., Solbiati, J., and Cronan, J. E., Jr (2000) Overproduction of acetyl-CoA carboxylase activity increases the rate of fatty acid biosynthesis in *Escherichia coli*. *J. Biol. Chem.* 275, 28593–28598.
- (30) Shi, S. B., Chen, Y., Siewers, V., and Nielsen, J. (2014) Improving production of malonyl coenzyme A-derived metabolites by abolishing Snf1-dependent regulation of Acc1. *mBio* 5, e01130-14.

- (31) Campbell, J. W., Morgan-Kiss, R. M., and Cronan, J. E. (2003) A new *Escherichia coli* metabolic competency: growth on fatty acids by a novel anaerobic beta-oxidation pathway. *Mol. Microbiol.* 47, 793–805.
- (32) Morgan-Kiss, R. M., and Cronan, J. E. (2004) The *Escherichia coli* fadK (ydiD) gene encodes an anaerobically regulated short chain acyl-CoA synthetase. *J. Biol. Chem.* 279, 37324–37333.
- (33) Dirusso, C. C., and Black, P. N. (2004) Bacterial long chain fatty acid transport: gateway to a fatty acid-responsive signaling system. *J. Biol. Chem.* 279, 49563–49566.
- (34) Ford, T. J., and Way, J. C. (2015) Enhancement of *E. coli* acyl-CoA synthetase FadD activity on medium chain fatty acids. *PeerJ.* 3, e1040.
- (35) Jarboe, L. R., Zhang, X., Wang, X., Moore, J. C., Shanmugam, K. T., and Ingram, L. O. (2010) Metabolic engineering for production of biorenewable fuels and chemicals: contributions of synthetic biology. *J. Biomed. Biotechnol.* 2010, 761042.
- (36) Monk, J. M., Charusanti, P., Aziz, R. K., Lerman, J. A., Premyodhin, N., Orth, J. D., Feist, A. M., and Palsson, B. O. (2013) Genome-scale metabolic reconstructions of multiple *Escherichia coli* strains highlight strain-specific adaptations to nutritional environments. *Proc. Natl. Acad. Sci. U. S. A.* 110, 20338–20343.
- (37) Clomburg, J. M., Blankschien, M. D., Vick, J. E., Chou, A., Kim, S., and Gonzalez, R. (2015) Integrated engineering of beta-oxidation reversal and omega-oxidation pathways for the synthesis of medium chain omega-functionalized carboxylic acids. *Metab. Eng.* 28, 202–212.
- (38) Torella, J. P., Ford, T. J., Kim, S. N., Chen, A. M., Way, J. C., and Silver, P. A. (2013) Tailored fatty acid synthesis via dynamic control of fatty acid elongation. *Proc. Natl. Acad. Sci. U. S. A.* 110, 11290–11295.
- (39) Jing, F. Y., Cantu, D. C., Tvaruzkova, J., Chipman, J. P., Nikolau, B. J., Yandea-Nelson, M. D., and Reilly, P. J. (2011) Phylogenetic and experimental characterization of an acyl-ACP thioesterase family reveals significant diversity in enzymatic specificity and activity. *BMC Biochem.* 12, 44.
- (40) Tee, T. W., Chowdhury, A., Maranas, C. D., and Shanks, J. V. (2014) Systems metabolic engineering design: fatty acid production as an emerging case study. *Biotechnol. Bioeng.* 111, 849–857.
- (41) Funai, N., Ohnishi, Y., Ebizuka, Y., and Horinouchi, S. (2002) Properties and substrate specificity of RppA, a chalcone synthase-related polyketide synthase in *Streptomyces griseus*. *J. Biol. Chem.* 277, 4628–4635.
- (42) Cheong, S., Clomburg, J. M., and Gonzalez, R. (2016) Energy- and carbon-efficient synthesis of functionalized small molecules in bacteria using non-decarboxylative Claisen condensation reactions. *Nat. Biotechnol.* 34, 556–561.
- (43) Baneyx, F. (1999) Recombinant protein expression in *Escherichia coli*. *Curr. Opin. Biotechnol.* 10, 411–421.
- (44) Sriubolmas, N., Panbangred, W., Sriurairatana, S., and Meevootisom, V. (1997) Localization and characterization of inclusion bodies in recombinant *Escherichia coli* cells overproducing penicillin G acylase. *Appl. Microbiol. Biotechnol.* 47, 373–378.
- (45) Mullick, A., Xu, Y., Warren, R., Koutroumanis, M., Guilbault, C., Broussau, S., Malenfant, F., Bourget, L., Lamoureux, L., Lo, R., Caron, A. W., Pilote, A., and Massie, B. (2006) The cumate gene-switch: a system for regulated expression in mammalian cells. *BMC Biotechnol.* 6, 43.
- (46) Schink, B., Philipp, B., and Muller, J. (2000) Anaerobic degradation of phenolic compounds. *Naturwissenschaften* 87, 12–23.
- (47) Neidhardt, F. C., Bloch, P. L., and Smith, D. F. (1974) Culture medium for enterobacteria. *J. Bacteriol.* 119, 736–747.
- (48) Bai, Y., Bi, H., Zhuang, Y., Liu, C., Cai, T., Liu, X., Zhang, X., Liu, T., and Ma, Y. (2015) Production of salidroside in metabolically engineered *Escherichia coli*. *Sci. Rep.* 4, 6640.
- (49) Bi, H., Bai, Y., Cai, T., Zhuang, Y., Liang, X., Zhang, X., Liu, T., and Ma, Y. (2013) Engineered short branched-chain acyl-CoA synthesis in *E. coli* and acylation of chloramphenicol to branched-chain derivatives. *Appl. Microbiol. Biotechnol.* 97, 10339–10348.
- (50) Clomburg, J. M., Vick, J. E., Blankschien, M. D., Rodriguez-Moya, M., and Gonzalez, R. (2012) A synthetic biology approach to engineer a functional reversal of the beta-oxidation cycle. *ACS Synth. Biol.* 1, 541–554.